LISTER G., KELTS K., CHEN K.Z., YU J.Q. and NIESSEN F., 1991. Lake Qinghai, China: closed-basin lake levels and the oxygen isotopic record for ostracoda since the latest Pleistocene. *Palaeogeogr. Palaeoclimatol. Palaeoecol.*, 84: 141-162.

THOMPSON L.G., MOSLEY-THOMPSON E., DAVIS E., BOLZAN J.F., DAI J., YAO T.D., GUNDESTRUP N., WU X., KLEIN L. and XIE Z., 1989. Holocene-late Pleistocene climatic ice core records from Qinghai-Tibet Plateau. *Science*, 246: 474-477.

THOMPSON L.G., YAO T., DAVIS M.E., HENDERSON K.A., MOSLEY-THOMPSON E., LIN P.-N., BEER J., SYNAL H.-A., COLE-DAI J. and BOLZAN J.F., 1997: Tropical climate instability: the last glacial cycle from a Qinghai-Tibet ice core. *Science*, 276: 1821-1825.

YU J.Q. and KELTS K.R., 2000. Abrupt changes in hydro-climatic conditions across the late glacial-to-Holocene transition on the N. E. Tibet-Qinghai Plateau: evidence from Qinghai Lake, China. *J. Paleolimnology*, (in review).

ZHOU W., DONAHUE D.J., PORTER S.C., JULL T.A., LI X., STUIVER M., AN Z., MATSUMOTO E. and DONG G., 1996. Variability of monsoon climate in East Asia at the end of the last glaciation. *Quat. Res.*, 46: 219-229.

Lake Level Fluctuation of Lake Lisan/Dead Sea and Lake Van (Turkey)

Günter LANDMANN, Michael KASELOW and Stephan KEMPE

Institute of Geology and Palaeontology, Schnittspahnstr. 9, 64287 Darmstadt, Germany

ABSTRACT. During the Last Glacial Maximum two prominent Near East depressions were filled with vast internal lakes: Lake Lisan/Dead Sea and Lake Van/East Anatolia. Both lakes left terraces composed of carbonate/detritus laminae and gypsum beds (in case of Lake Lisan). Here we present a study of geochemistry, mineralogy and sedimentology from two sites on the Jordan side of the Dead Sea rift valley. Elemental distribution was investigated within the finely laminated sediments by microprobe. The 'normal' sedimentation cycle is characterised by alternating clay and aragonite layers. In Lake Lisan periods of drought are identified by annual triplets of clay, aragonite and gypsum. ^{14}C-dates yield information about past lake levels. Comparison of lake level fluctuations between Lakes Lisan and Van revealed equivalent amplitudes, but the simultaneity of their phases still has to be shown.

KEY WORDS: palaeoclimate, varves, lake level, Lake Lisan, Lake Van.

Introduction

Between 70 and 15 ka the Dead Sea rift was occupied by a large, saline lake: Lake Lisan (e.g. Kaufmann, 1971; Schramm, 1997). It left terraces of up to 50 m thick laminated, i.e. varved, marl deposits (the Lisan Formation) (Begin et al., 1974). They rest unconformably on either older lacustrine sediments or bedrock of various age. Laminae alternate between light aragonite and dark detrital layers (e. g. Stein et al., 1997). Holocene sediments, up to 20 m thick, occur in fan delta regions near the Dead Sea shore consisting of detrital clay and authigenic aragonite as well (Migowski et al., 1998).

Methods and material studied

Two profiles were sampled. Profile LSM1 (32°00.2'N, 35°32.3'E) is situated about 7 km NW of the city of Karama. Here, the Jordan river has cut through over 50 m of deposits. The profile top is at 305 m below m.s.l., but patches of sediment and microbialites occur nearby as high as 280 m below m.s.l.. Profile LSM2 (31°17.3'N, 35°28.1'E, top at 370 m below m.s.l.) is located on the Lisan Peninsula, the type locality of the Lisan Marls. Two sample series were collected from the upper 26 m of each profile: a set of ca. 40 discrete samples for geochemical analyses and a continuous profile - using metal boxes overlapping each other - for the preparation of thin-sections and polished plates. Set 1 was used to conduct X-ray diffraction (XRD) and CNS-analyses. Distribution of Si, Al, Ca, Mg, S, K and Fe within the varves were studied on six thin-sections using a microprobe.

Results and discussion

Fig. 1 shows the lithology, chronology and geochemistry of the two profiles. The upper 10 m of LSM1 consist of dark laminated clay and silt, intercalated by non-laminated sections with several sand layers. Whitish coloured, laminated clay and silt mark a thin horizon at 2 m and a thick one from 10 to 21 m. Within the latter, sections with deformed lamination caused by slumping are observed. These occur preferentially below layers with elevated detritus content and may be caused by earthquakes (seismites, Marco et al., 1996). During an earthquake sediments are consolidated, causing the pore water to move upward. This flux may be blocked by the detritus rich layers leading to a pore water supersaturation and hence to sliding planes. Severely slumped sections, sand layers and turbidites mark the dark sediments of the lowest profile section.

The most striking feature of profile LSM2 is the alternation of horizons dominated by gypsum or aragonite. Under the arid climate of the Lisan peninsula the gypsum layers are resistant to erosion forming flat, step-like platforms promi-

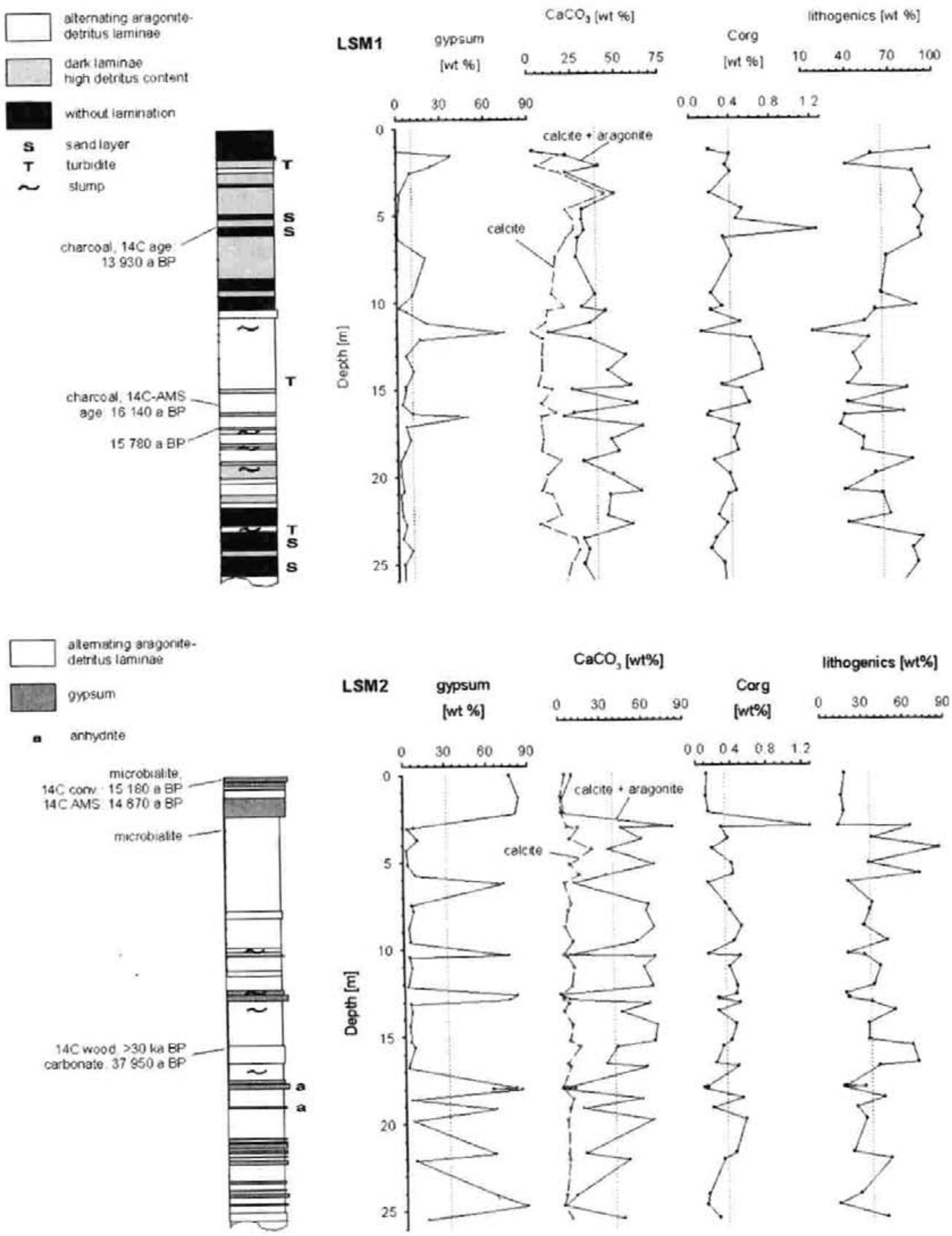

Fig. 1. Lithology, chronology and geochemical results of profile LSM1 and LSM2. Results of sulphur and inorganic carbon analyses were recalculated as gypsum and $CaCO_3$, respectively. The distribution of calcite and aragonite was distinguished by fitting their peak height, obtained from semi-quantitative XRD-analyses, versus the quantitative $CaCO_3$-analyses with a multivariate general linear hypothesis resulting in a R^2 of 0.87 and 0.95 for LSM1 and LSM2, respectively. Lithogenic-content was calculated as 100 - gypsum -aragonite - C_{org} (as CH_2O). Vertical dotted line represents mean values.

nent at 18 and 12.5 m and at the top of the profile. Here, the gypsum is partly covered with benches of arenitic limestone of microbialitic origin dated to 15,180 ± 140 years BP by conventional and to 14,670 ± 70 years BP by AMS ^{14}C-method. Except in some massive horizons containing nearly exclusively gypsum, aragonite as well as gypsum alternate with detritus laminae at a millimetre scale throughout the entire profile.

Additionally low Mg-calcite, halite, quartz and feldspars were identified by XRD-analysis. The positive correlation between the concentrations of quartz, undoubtedly of allochthonous origin, calcite and feldspars suggest that these minerals are also allochthonous, in contrast to aragonite and gypsum which are precipitates from the lake water column (e.g. Yechieli et al., 1991). Gypsum horizons, representing drought periods (e.g. Stein et al., 1997), were predominately followed by layers with lithogenic detritus indicating flushing and a low lake level. Anhydrite was found only in 3 samples of LSM2 but its environmental significance remains unclear. At 3 m profile depth microbialites were found, they can be clearly distinguished from the normal sediment by their high content of organic carbon and aragonite. Overall the proportion of autochthonous minerals is higher in LSM2, while lithogenics prevail in LSM1. As aragonite is an indicator for lake deposits, the facies of the sections 3–10 m and > 23 m of LSM1 were shallow limnic or deltaic.

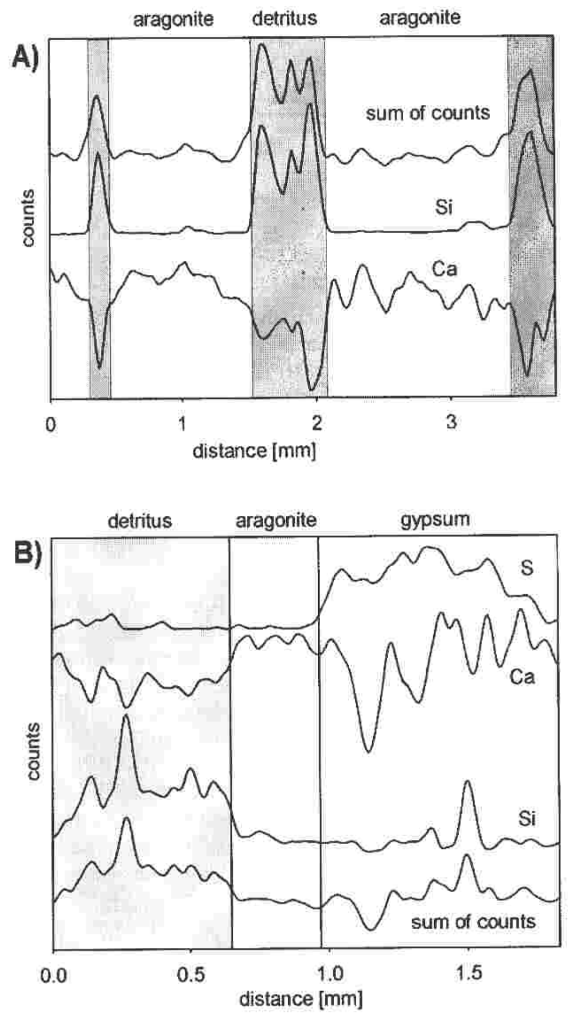

Fig. 2. Element distribution within varves measured by microprobe. Data were smoothed by a running average over three values. Top points to the right. a) Alternating aragonite/detritus laminae of LSM2 at a depth of 14.1 m. Vertical resolution is 47 measurements per mm. b) Lamination within a gypsum dominated sequence of LSM1 at a depth of 11.6 m, scanned with a resolution of 131 measurements per mm.

The ^{14}C-ages are given without calibration to allow comparison with data from the literature. Depending on the age and on the calibration curve used, 1–3 ka have to be added to the ^{14}C-ages obtained for organic carbon. The reservoir effect for aragonite ranges from 3.4 to 5 ka (average 4 ka, see Schramm, 1997). The sedimentation rate resulting from the two dated layers of LSM2 amounts to ca. 0.8 mm per year. This is in accordance with the first varve count conducted during sampling. Dating results from LSM1 are less clear. Two dates from a depth of ca. 16 m do not follow stratigraphic order. Also the time difference between the 5.6 m and the 16 m samples are less than half that of the varve count. Both inaccuracies could indicate redeposition of charcoal or slumping. To clarify this OSL-dating is in progress.

Microprobe analysis shows positive correlation between Al, K, Mg, Si and Fe. Their peaks, representing the detrital phase, is normally followed by a Ca-peak (Fig. 2a). The latter shows saw-tooth pattern with a sudden onset and a slow decline. In sections with high S contents, however, three phases can be identified, with a sulfate phase following the detrital and aragonitic layers (Fig. 2b). Upon evaporation in summer first the $CaCO_3$ saturation is surpassed before that for gypsum. The scatter of the Ca-curve with the onset of the S-peak is caused by weak emissions (see sum of counts: Fig. 2b).

Several attempts were made to reconstruct the lake level curves of Lake Lisan and the Dead Sea (Fig. 3). There is sufficient agreement on the amplitudes of Dead Sea level changes but there are discrepancies as to their timing due the differing interpretations of the ^{14}C-dates. Timing and amplitude of Lake Lisan fluctuations is still intensively discussed. Re-examination of seismic reflection profiles of the Dead Sea basin revealed five cycles of low- and high-stands with a major erosional event at sequence 2, which is correlated to channel incisions at the final retreat of Lake Lisan (Niemi, 1997). Based on the observation of a drainage system presently underwater, Neev and Emery (1967) suggested that the lake level dropped to about 700 m below m.s.l. during the transition between Lake Lisan and the Dead Sea. A hiatus in a sediment core retrieved from the Zeelim plateau (-394 m m.s.l.) indicates an erosional (or non-depositional) period from 21.1–11.3 ka followed by an arid phase recorded by a 6.5 m thick layer of halite that ended prior to 8.4 ka (Yechieli et al., 1991).

For comparison the lake level curve of Lake Van, located ca. 1000 km NE of the Dead Sea, is given (Fig. 3). Its reconstruction is based on 19 sediment cores, lake terraces and wave-cut benches (Landmann et al., 1996a). The time scale of the record is based on a varve chronology, which places the transition Pleistocene/Holocene at 10.9 ka cal. (Landmann et al., 1996b). Between 19 ka cal. and 15 ka cal. Lake Van fell dry, marking a reduction of the lake level by 500 m. As it is unlikely that such drastic event is based on regional climate conditions only, it must be assumed that the dry-up of both lakes happened simultaneously.

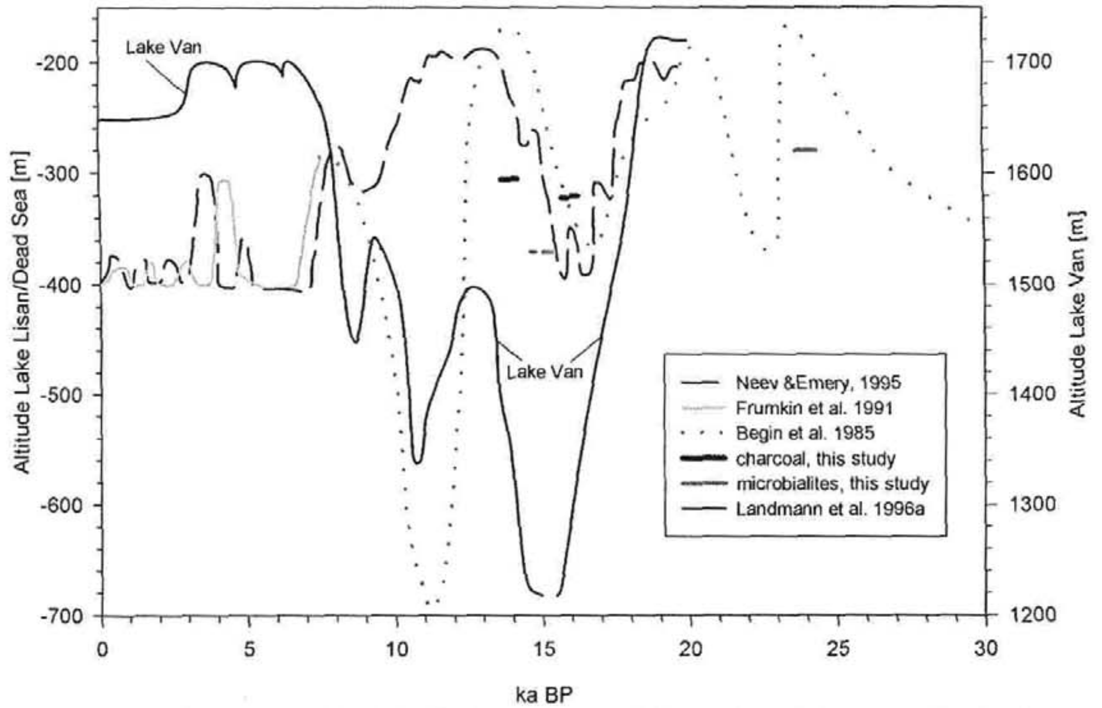

Fig. 3. Reconstruction of the level of Lake Lisan/Dead Sea according to different authors and of that of Lake Van (Landmann et al., 1996a). Lake Van fell dry at around 15 ka BP. The time scale succeeding that hiatus is based on varve chronology, older section of curve is based on calibrated ^{14}C ages. Uncorrected ^{14}C dates (see text) on charcoal and carbonate of microbialites and the related level of Lake Lisan are included.

Acknowledgements

The field work for this study was conducted in co-operation with the National Resources Authority of Jordan. The project is funded by the German Research Council (DFG Ke 287/16-(1-3)).

References

BEGIN Z.B., EHRLICH A. and NATHAN Y., 1974. Lake Lisan, the Pleistocene precursor of the Dead Sea. *Geol. Society of Israel*, 63: 30.

BEGIN Z.B., BROECKER W., BUCHBINDET B., DRUCKMAN Y., KAUFMAN A., MAGARIT, M. and NEEV D., 1985. Dead Sea and Lake Lisan levels in the last 30,000 years. *Geol. Survey of Israel, Preliminary report* 29/85: 18.

FRUMKIN A., MAGARITZ M., CARMI I. and ZAK I., 1991. The Holocene climatic record of the salt caves of Mount Sedom, Israel. *Holocene*, 1: 191-200.

KAUFMANN A., 1971:U-series, dating of Dead Sea basin carbonates. *Geochim. Cosmochim. Acta*, 35: 1269-1281.

LANDMANN G., REIMER A. and KEMPE S., 1996a. Climatically induced lake level changes at Lake Van, Turkey during the Pleistocene/Holocene transition. *Global Biochem. Cycles*, 10/4: 797-808.

LANDMANN G., REIMER A., LEMCKE G. and KEMPE S., 1996b. Dating late glacial abrupt changes in the 14,570 yr long continuous varve record of Lake Van, Turkey. *Palaeogeogr. Palaeoclimatol. Palaecol.*, 122: 107-118.

MARCO S., STEIN M., AGNON A. and RON H., 1996. Long-term earthquake clustering: a 50,000-year paleoseismic record in the Dead Sea Graben. *Journal of Geophysic. Research*, 101/B3: 6179-6191.

MIGOWSKI C., KEN-TOR R., NEGENDANK J.F.W., STEIN M. and MINGRAM J., 1998. Post-Lisan record documented in sediment sequences from the western shore area and the central basin of the Dead Sea. Terra Nostra 98/6, 3rd ELDP Workshop, Ptolemais, Greece, pp.100-102.

NEEV D. and EMERY K., 1967. The Dead Sea: Depositional processes and environments of evaporites. *Geol. Survey oj Israel Bulletin*, 41.

NIEMI T.M., 1997. Fluctuations of Late Pleistocene Lake Lisan in the Dead Sea Rift. In: T.M. NIEMI, Z. BEN-AVRAHAM AND J.R. JOEL (Editors), The Dead Sea, the Lake and its Setting. *Oxford Monographs on Geology and Geophysics*, 36: 226-236.

SCHRAMM A., 1997. Uranium series and 14C dating of Lake Lisan (Paleo-Dead Sea) sediments: implications for 14C time-sale calibration and relation to global paleoclimate. Ph.D. Thesis, Univ. Goettingen, Germany.

STEIN M., STARINSKY A., KATZ A., GOLDSTEIN S.L., MACHLUS M. and SCHRAMM A., 1997. Strontium isotopic, chemical, and sedimetological evidence for the evolution of Lake Lisan and Dead Sea. *Geochim. Cosmochim. Acta*, 61: 3975-3992.

YECHIELI Y., MAGARITZ M., LEVI Y., WEBER U., KAFRI U., WOELFLI W. and BONANI G., 1991. Late Quaternary geological history of the Dead Sea area, Israel. *Quaternary Research*, 39: 59-67.